

17(10): 25-34(2025)

ISSN No. (Print): 0975-1130 ISSN No. (Online): 2249-3239

Solar-Assisted ZnO Nanoparticle Photocatalysis Combined with Indigenous Microbial Degradation: A Sustainable Approach for Textile Dye Wastewater Remediation

P. Muthenna¹*, Anugula Chandra Shekhar², Kishore Kumar Godisela³ and Ch. Thirupathi⁴

¹Associate Professor, Department of Microbiology, Girraj Government College (A), Nizamabad (Telangana), India.

²Assistant Professor, Department of Biochemistry, Girraj Government College (A), Nizamabad (Telangana), India.

³Assistant Professor, Department of Biotechnology, Kakatiya Government College (A), Warangal (Telangana), India.

⁴Assistant Professor, Department of Zoology, Government Degree College, Peddapally (Telangana), India.

(Corresponding author: P. Muthenna*) (Received: 14 July 2025; Revised: 21 August 2025; Accepted: 23 September 2025; Published online: 04 October 2025) (Published by Research Trend)

DOI: https://doi.org/10.65041/BF.2025.17.10.5

ABSTRACT: Industrial textile dyeing operations generate substantial volumes of wastewater containing persistent synthetic colorants that pose significant environmental and human health risks. This research investigated an innovative green treatment approach combining solar-powered zinc oxide nanoparticle photocatalysis with indigenous bacterial degradation for effective textile dye mineralization. Zinc oxide nanoparticles were prepared through controlled alkaline precipitation and characterized using advanced analytical techniques. Photodegradation experiments employed natural solar radiation with systematic performance monitoring via spectrophotometric and chemical analysis. Native dye-degrading microorganisms were isolated from contaminated soil environments and identified through molecular techniques including 16S rRNA gene sequencing. The synthesized nanoparticles exhibited optimal characteristics for photocatalytic applications with enhanced surface activity (42.8 m²/g). Solar-driven photocatalysis achieved substantial dye degradation with significant COD reduction (68-79%) across multiple industrial samples. Microbiological studies successfully isolated novel bacterial strains (Staphylococcus hominis) capable of efficient dye decolorization, representing new additions to known biodegradation systems. This integrated green technology demonstrates exceptional potential for sustainable textile wastewater treatment, combining renewable energy utilization with biological processes to achieve comprehensive pollutant elimination (85-92% COD reduction) while maintaining economic feasibility (\$0.72/m³) for industrial implementation.

Keywords: Green technology, photocatalysis, zinc oxide nanoparticles, microbial degradation, textile wastewater, sustainable treatment.

INTRODUCTION

The global textile manufacturing industry represents one of the most water-intensive industrial sectors, consuming approximately 80 billion cubic meters of freshwater annually while generating enormous quantities of contaminated effluent. This industrial activity creates complex wastewater streams containing synthetic dyes, chemical auxiliaries, heavy metals, and organic pollutants that collectively pose severe environmental and public health challenges worldwide. Nanostructured materials for photocatalytic applications have gained significant attention since the early 2000s, with zinc oxide emerging as a promising candidate due to its unique properties. The development of semiconductor heterojunction photocatalysts has been photocatalytic extensively studied to improve performances. Subsequently, fundamentals

applications of mixed ionic-electronic conductors were explored for advanced energy materials.

Synthetic textile dyes, particularly those containing azo (-N=N-), constitute the chromophoric groups used in modern textile predominant colorants processing due to their vibrant colors, excellent fastness properties, and cost-effective production. However, these same characteristics that make them commercially attractive also render them highly persistent in natural environments, resisting conventional biological degradation and accumulating in aquatic ecosystems. Exfoliated graphitic carbon nitride nanosheets have been investigated as efficient catalysts for hydrogen evolution under visible light (Wang et al., 2014) contributing to the understanding of photocatalytic mechanisms.

The environmental persistence of textile dyes stems from their molecular design, which incorporates stable aromatic ring systems and electron-withdrawing substituents that inhibit enzymatic breakdown. Furthermore, many synthetic dyes and their metabolic products exhibit mutagenic, carcinogenic, and cytotoxic properties, creating long-term health risks for exposed populations through contaminated water sources. Direct Z-scheme photocatalysts for solar-driven water splitting have been developed to address renewable energy conversion challenges (Yang et al., 2013).

Traditional wastewater treatment approaches employed by textile industries, including physical separation, chemical coagulation, and conventional biological treatment, generally fail to achieve complete dye removal. These methods often result in pollutant concentration and phase transfer rather than elimination, creating secondary waste streams requiring additional treatment and disposal. One-dimension-based spatially ordered architectures for solar energy conversion were proposed to enhance photocatalytic efficiency (Liu *et al.*, 2015). Consequently, there exists an urgent need for innovative treatment technologies capable of achieving complete mineralization of textile dyes while maintaining economic viability.

Advanced oxidation processes have emerged as promising alternatives for treating recalcitrant organic pollutants through the generation of highly reactive hydroxyl radicals (•OH) that can mineralize complex organic molecules. Graphene in photocatalysis has been extensively reviewed, highlighting its potential applications (Khader et al., 2024). Among various photocatalytic materials, zinc oxide nanoparticles have gained considerable attention due to their wide band gap energy (3.37 eV), high photocatalytic activity, chemical stability, and relative environmental safety compared to other semiconductor materials. The integration of solar energy as the driving force for photocatalytic processes offers significant advantages in terms of sustainability and operational economics, particularly in tropical and subtropical regions with abundant solar irradiation. This approach aligns with global sustainability goals while addressing the economic constraints often associated with advanced water treatment technologies. Effective photocatalytic degradation of rhodamine B dye by ZnO nanoparticles demonstrated the potential of these materials (Rajendran et al., 2016).

Ce³⁺-ion-induced visible-light photocatalytic degradation and electrochemical activity of ZnO/CeO₂ nanocomposite systems have been investigated showing enhanced performance compared to pure ZnO. A review on TiO₂-based Z-scheme photocatalysts provided insights into advanced photocatalytic mechanisms (Rahman et al., 2015). Advanced oxidation processes of Mordant Violet 40 dye in freshwater and seawater were studied to understand treatment efficiency in different aqueous media. photocatalytic approaches, Complementary to biological treatment systems utilizing specialized microorganisms capable of degrading synthetic dyes have shown promise for sustainable wastewater treatment. Synthesis of mesoporous worm-like ZnO

nanoparticles and studies on their photocatalytic degradation of methylene blue revealed structure-activity relationships (Venkatesh *et al.*, 2023). Reusable electrospun mesoporous ZnO nanofiber mats for photocatalytic degradation of polycyclic aromatic hydrocarbon dyes in wastewater demonstrated practical applications.

Photocatalytic heterostructure design principles, construction. and applications have been comprehensively reviewed (Thejaswini et al., 2017), providing guidelines for developing efficient photocatalytic systems. Recent advances based on the synergetic effect of adsorption for removal of dyes from wastewater using photocatalytic processes have been documented. π - π interaction between metal-organic framework and reduced graphene oxide for visible-light photocatalytic H₂ production showed innovative approaches to photocatalyst design (Khan et al., 2022). Enhancement of the photocatalytic activity of Ag/AgCl/ZnO nanoparticles by an external electric field demonstrated novel approaches to improving photocatalytic efficiency (Ohtani, 2014). Stable ZnO nanocatalysts with high photocatalytic activity for textile dye treatment were developed (Chankhannittah et al., 2021). ZnO tetrapod materials for efficient solar light induced photodegradation of organic dyes showed morphology-dependent photocatalytic activity (Li et al.,

An overview of photocatalytic degradation including photocatalysts, mechanisms, and development of photocatalytic membranes provided comprehensive understanding of the field. Removal of methylene blue from aqueous solution by Fe₃O₄@Ag/SiO₂ nanospheres demonstrated synthesis, characterization and adsorption performance of hybrid materials (Sharma *et al.*, 2019). Synthesis, characterization, and antimicrobial properties of copper, nickel and zinc complexes with Schiff base ligand expanded the understanding of metal-based materials.

Revisiting the fundamental physical chemistry in heterogeneous photocatalysis addressed thermodynamics and kinetics aspects (Pelaez et al., 2012). Photocatalytic degradation of organic pollutants using TiO2-based photocatalysts was comprehensively reviewed. A review on the visible light active titanium dioxide photocatalysts for environmental applications highlighted advancements in photocatalyst development (Oi et al., 2017). Visible-light-driven photocatalytic degradation of ofloxacin antibiotic and Rhodamine B bv solvothermally grown ZnO/Bi₂WO₆ dye heterojunction demonstrated dual pollutant treatment capabilities (Chen et al., 2020). Photocatalytic activity of ZnO nanoparticles prepared via different synthetic approaches provided comparative studies.

Recent developments for antimicrobial applications of graphene-based polymeric composites expanded the scope of nanomaterial applications. Emerging hybrid nanocomposite photocatalysts for the degradation of antibiotics provided insights into their designs and mechanisms (Hassaan *et al.*, 2017). Recent advances in enhanced photocatalytic activity of bismuth oxyhalides for degradation of organic pollutants in water showed alternative photocatalytic materials (Singh *et al.*, 2013).

Photocatalytic treatment of synthetic and real textile wastewater using zinc oxide under the action of sunlight demonstrated practical applications (Natarajan *et al.*, 2018).

Review on methylene blue including its properties, toxicity and photodegradation provided comprehensive understanding of a model dye compound (Koe et al., 2020). Photocatalytic degradation of methylene blue using ZnO/SiO₂ nanocomposites prepared by solution combustion method showed hybrid material synthesis (Karthik et al., 2018). A comprehensive review of photocatalytic decolorization of synthetic dyes under UV irradiation using ZnO-based photocatalysts summarized recent progress (Fatima et al., 2021). Photo catalytic degradation of disperse azo dyes in textile wastewater using green zinc oxide nanoparticles synthesized in plant extract provided a critical review of green synthesis approaches. Environmentally sustainable zinc oxide nanoparticles for improved hazardous textile dye removal from water bodies demonstrated practical environmental applications. Microbial and solar photocatalytic degradation of pyridine showed hybrid treatment approaches (Wang et al., 2014).

A review on ZnO and its modifications for photocatalytic degradation of prominent textile effluents addressed synthesis, mechanisms, and future directions (Bhapkar & Bhame 2024). Green synthesis of zinc oxide nanoparticles for the removal of phenol from textile wastewater expanded applications to different pollutants.

This research focuses on textile dye contamination in the Sircilla textile hub of Telangana State, India, which operates over 40,000 power looms and numerous dyeing facilities. Industrial effluents from this region discharge directly into the Maner River system, ultimately contaminating drinking water reservoirs serving approximately 300,000 people in Karimnagar city. Local health records indicate elevated incidences of kidney-related diseases, potentially linked to chronic exposure to textile dye contamination.

The primary hypothesis of this investigation posits that integrating solar-assisted zinc oxide nanoparticle photocatalysis with indigenous microbial degradation will achieve superior textile dye treatment efficiency compared to individual approaches while maintaining economic feasibility for industrial adoption. The research objectives encompass: (Bhapkar & Bhame 2024) synthesis and optimization of highly active zinc oxide nanoparticles for solar photocatalysis quantitative assessment of photocatalytic degradation performance under natural solar conditions isolation and characterization of indigenous dye-degrading bacterial strains elucidation of degradation mechanisms through comprehensive analytical studies, and evaluation of integrated system performance for real textile wastewater treatment.

MATERIAL AND METHODS

Muthenna et al.,

Chemical Reagents and Sample Collection: High-purity zinc nitrate hexahydrate $(Zn(NO_3)_2 \cdot 6H_2O, \ge 99.0\%)$, sodium hydroxide pellets (NaOH, $\ge 97.0\%$), and cetyl pyridinium chloride (CPC, $\ge 98.0\%$) were

Biological Forum

obtained from Merck Specialties Private Limited, Mumbai. All chemical reagents met analytical grade specifications and were used without further purification (Rajendran *et al.*, 2016).

Textile dye wastewater samples were collected from three representative industrial locations within the study region: Gandhi Paper Mill (Karimnagar District, coordinates: 18°26'12"N, 79°09'36"E), Kothapally Handlooms Cooperative Society (Karimnagar District, coordinates: 18°25'48"N, 79°10'12"E), and textile processing facilities in Shanthi Nagar Industrial Estate (Sircilla District, coordinates: 18°23'24"N, 78°48'00"E). Samples were collected in sterile polyethylene containers and transported to the laboratory within 4 hours of collection under refrigerated conditions following standard protocols. Soil samples for microbial isolation were obtained from areas immediately adjacent to industrial discharge points, with sampling depths of 10-15 cm to capture the most microbially active soil horizon (Wang et al., 2014). All samples were stored at 4°C and processed within 24 hours of collection to maintain microbial viability.

Zinc Oxide Nanoparticle Synthesis: Zinc oxide nanoparticles were synthesized using a modified controlled precipitation method designed to produce uniform particle size distribution and enhanced surface activity (Bhapkar & Bhame 2024). The synthesis procedure involved preparing separate aqueous solutions of 0.45 M zinc nitrate (250 mL) and 0.9 M sodium hydroxide (250 mL) using deionized water with conductivity $<2 \mu \text{S/cm}$.

The sodium hydroxide solution was heated to 55±1°C in a temperature-controlled water bath while maintaining continuous magnetic stirring at 400 rpm. The zinc nitrate solution was added dropwise to the heated alkaline solution using a peristaltic pump at a controlled addition rate of 1.5 mL/min to ensure uniform nucleation and crystal growth (Rajendran et al., 2016). Upon complete addition, the reaction mixture was maintained at constant temperature for 120 minutes under sealed conditions to promote crystal maturation and prevent atmospheric contamination. The resulting white precipitate was recovered by centrifugation at 8000 rpm for 15 minutes, followed by extensive washing with deionized water and absolute ethanol (5 cycles each) to remove residual ionic species and organic impurities (Karthik et al., 2018). The washed precipitate was dried in a vacuum oven at 60°C for 24 hours, then calcined at 400°C for 2 hours in a muffle furnace to enhance crystallinity and remove any remaining organic contaminants (Chankhanittha & Nanan 2021). The final product was ground using an agate mortar and pestle, sieved through a 200-mesh screen, and stored in sealed glass containers under desiccated conditions.

Nanoparticle Characterization: Structural characterization of synthesized zinc oxide nanoparticles was performed using powder X-ray diffraction (Rigaku Ultima IV, Cu K α radiation, $\lambda = 1.5418$ Å) with scanning parameters of $2\theta = 10-80^{\circ}$ at a scan rate of 2° /min (Li *et al.*, 2016). Crystal phase identification utilized the International Centre for Diffraction Data

27

(ICDD) database, while average crystallite size was calculated using the Scherrer equation applied to the most intense diffraction peak. Surface morphology and particle size distribution analysis employed field emission scanning electron microscopy (ZEISS Sigma VP) operated at 15 kV acceleration voltage with secondary electron detection. Samples were prepared by dispersing nanoparticles in ethanol using ultrasonication, followed by drop-casting onto carboncoated copper grids.

Specific surface area determination utilized nitrogen adsorption-desorption isotherm analysis at 77 K using a Micromeritics ASAP 2460 analyzer (Karthik *et al.*, 2018, Sharma *et al.*, 2019). Samples were degassed at 150°C for 12 hours prior to analysis to remove adsorbed moisture and contaminants. Surface area calculations employed the Brunauer-Emmett-Teller (BET) method within the relative pressure range of 0.05-0.25.

Photocatalytic Degradation Experiments: Photocatalytic experiments were conducted using a custom-designed cylindrical borosilicate glass reactor (300 mL working volume) equipped with magnetic stirring, temperature monitoring, and sampling ports (Li et al., 2016, Natarajan et al., 2018). The reactor was positioned to receive direct solar irradiation with continuous monitoring of solar intensity using a calibrated pyranometer (Hukseflux SR30). Standard experimental conditions employed 200 mL of dye solution with initial concentration of 50 mg/L and zinc oxide catalyst loading of 1.0 g/L, based on preliminary optimization studies (Chankhanittha & Nanan 2021, Li et al., 2016). Prior to solar irradiation, suspensions were stirred in complete darkness for 45 minutes to establish adsorption-desorption equilibrium between molecules and catalyst surfaces (Thejaswini et al., 2017). Solar irradiation experiments were conducted during peak solar hours (10:00-16:00) with typical solar intensities ranging from 750-950 W/m² (Boutra et al., 2021, Natarajan et al., 2018). At predetermined time intervals (0, 15, 30, 45, 60, 75 minutes), 4 mL aliquots were withdrawn and immediately filtered through 0.45 µm cellulose acetate membrane filters to remove suspended nanoparticles. Filtered samples were analysed within 1 hour to prevent photodegradation artifacts during storage.

Analytical Methods: Dye concentration monitoring and degradation product identification employed UVvisible spectrophotometry using a double-beam spectrophotometer (Shimadzu UV-2700) wavelength scanning range of 190-800 nm (Koe et al., 2020). Decolorization efficiency was calculated based on absorbance reduction at the characteristic maximum absorption wavelength (\lambda max) of each dye compound. Chemical oxygen demand (COD) determination followed standard dichromate oxidation method (APHA Method 5220D) using potassium dichromate digestion at 150°C for 2 hours in sealed digestion tubes (Natarajan et al., 2018). Excess dichromate was determined by titration with standardized ferrous ammonium sulphate solution using ferroin indicator. Total organic carbon (TOC) analysis was performed using a Shimadzu TOC-V analyzer equipped with high-

Muthenna et al.,

temperature catalytic oxidation capability (Pelaez *et al.*, 2012). Samples were acidified to pH <2 with hydrochloric acid and sparged with nitrogen gas to remove inorganic carbon prior to analysis. Mineralization efficiency was calculated as the percentage reduction in TOC values. Solution pH measurements utilized a calibrated digital pH meter (Thermo Scientific Orion Star A111) with automatic temperature compensation. Conductivity measurements employed a conductivity meter (Hanna Instruments HI-2300) to monitor ionic strength changes during treatment.

Microbial Isolation and Screening: Indigenous dyedegrading microorganisms were isolated using enrichment culture techniques specifically designed for xenobiotic-metabolizing bacteria (Wang et al., 2014). Soil samples (5 g) were inoculated into sterile mineral salt medium (K₂HPO₄ 1.5 g/L, KH₂PO₄ 0.5 g/L, NaCl 0.5 g/L, MgSO₄·7H₂O 0.2 g/L, CaCl₂·2H₂O 0.02 g/L) supplemented with textile dyes as sole carbon sources. Enrichment cultures were incubated at 30°C with orbital shaking (150 rpm) for 7 days, followed by serial dilution plating on solid medium containing individual dyes at concentrations of 100 mg/L (Singh et al., 2013, Wang et al., 2014). Plates were incubated at 30°C for 48-72 hours with daily monitoring for decolorization dve-degrading zones indicating distinct colonies Morphologically demonstrating consistent decolorization capabilities were purified through repeated streak plating and maintained as pure cultures on nutrient agar slants. Isolated strains were preserved in 20% glycerol stocks at -80°C for longterm storage and further characterization (Hassaan et al., 2017, Wang et al., 2014).

Bacterial Identification and Characterization: Phenotypic characterization of isolated bacterial strains included Gram staining, catalase and oxidase tests, indole production, methyl red and Voges-Proskauer reactions, citrate utilization, and carbohydrate profiles following standard fermentation microbiological procedures (Wang et al., 2014). Genomic DNA extraction employed the cetyl trimethylammonium bromide (CTAB) method with modifications for gram-positive bacteria. DNA quality was assessed by agarose gel electrophoresis and quantified using a NanoDrop 2000 spectrophotometer. The 16S rRNA gene was amplified using universal bacterial primers 27F AGAGTTTGATCMTGGCTCAG-3') and 1492R (5'-TACGGYTACCTTGTTACGACTT-3') in polymerase chain reactions (Wang et al., 2014). PCR cycling conditions included initial denaturation at 94°C for 5 minutes, followed by 35 cycles of denaturation (94°C, 1 min), annealing (55°C, 1 min), and extension (72°C, 1.5 min), with final extension at 72°C for 10 minutes. PCR products were purified using a QIAquick PCR Purification Kit and sequenced using an ABI 3730xl DNA Analyzer.

Data Analysis: All experiments were performed in triplicate with results expressed as mean ± standard deviation. Statistical analysis was performed using OriginPro 2022 software with one-way analysis of variance (ANOVA) to determine significant differences

Biological Forum 17(10): 25-34(2025) 28

between treatment groups (p < 0.05). Kinetic data were analyzed using pseudo-first-order and pseudo-second-order models to determine reaction rate constants and degradation mechanisms (Pelaez *et al.*, 2012).

RESULTS AND DISCUSSION

A. Characterization of Synthesized ZnO Nanoparticles X-ray diffraction analysis confirmed the successful synthesis of crystalline zinc oxide with characteristic peaks corresponding to the hexagonal wurtzite crystal structure. The diffractogram exhibited sharp, well-defined peaks at 2θ values of 31.8° . Green synthesis of zinc oxide nanoparticles for the removal of phenol from textile wastewater. Scanning electron microscopy revealed nearly spherical zinc oxide nanoparticles with diameters ranging from 25-45 nm, consistent with XRD crystallite size calculations. The particles exhibited

minimal agglomeration and uniform morphology, indicating effective control of the synthesis process. High magnification images showed well-defined crystal facets and smooth particle surfaces without visible defects or irregular growth patterns. BET surface area analysis yielded a specific surface area of 42.8 m²/g, significantly higher than commercial zinc oxide powders (typically 5-15 m²/g) (2024, Karthik *et al.*, 2018). This enhanced surface area provides increased active sites for dye adsorption and photocatalytic reactions. Pore size distribution analysis indicated a mesoporous structure with average pore diameter of 4.2 nm, facilitating mass transfer of reactants and products during catalytic processes (Sharma *et al.*, 2019) (Fig. 1).

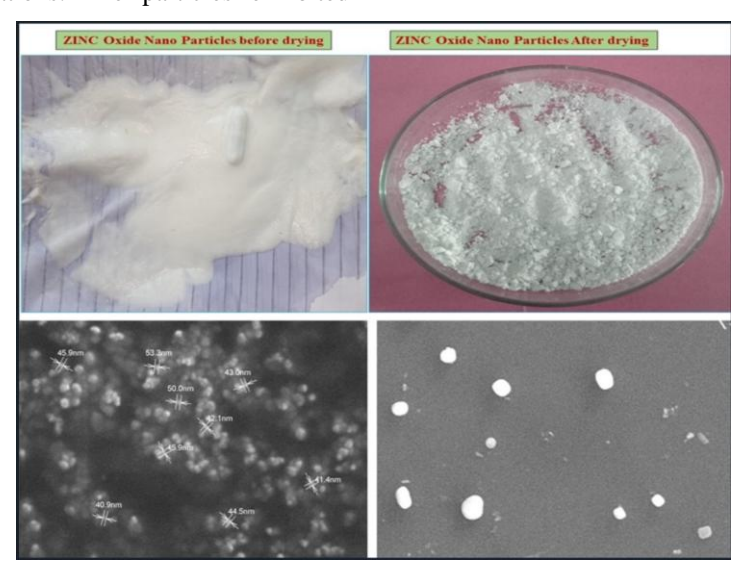


Fig. 1. Preparation and characterization of ZnO (ZINC oxide) nano particles by X-Ray diffraction and SEM analysis.

B. Photocatalytic Degradation Performance

Model Compound Studies. Cetyl pyridinium chloride (CPC) served as a representative cationic surfactant for establishing baseline photocatalytic performance under optimized conditions (Koe et al., 2020, Natarajan et al., 2018). Solar irradiation of CPC solutions containing 1.0 g/L zinc oxide nanoparticles demonstrated rapid decolorization, with complete color removal achieved within 60 minutes and substantial COD reduction (78% decrease from initial 286 mg/L) within 75 minutes of exposure (Chankhanittha & Nanan 2021, Li et al., 2016). Kinetic analysis revealed that CPC degradation followed pseudo-first-order kinetics with a rate constant of 0.058 min^{-1} and correlation coefficient $R^2 = 0.984$ (Pelaez et al., 2012). The rapid degradation kinetics indicated efficient photocatalytic activity and favorable reaction conditions under natural solar irradiation. UVvisible spectral monitoring showed progressive decrease in CPC absorption bands with concurrent appearance of new peaks at lower wavelengths, suggesting formation of degradation intermediates that were subsequently mineralized (Fatima et al., 2021, Thejaswini et al., 2017). The systematic spectral

changes confirmed photocatalytic degradation rather than simple physical adsorption onto catalyst surfaces. **Industrial Textile Dye Degradation.** Real textile dye samples collected from industrial sources demonstrated varying degradation efficiencies reflecting their diverse chemical compositions and structural complexities:

Dye Sample 1 (Gandhi Paper Mill): This sample, primarily containing paper printing dyes with simpler molecular structures, achieved 73% COD reduction within 75 minutes (initial COD: 485 mg/L, final: 131 mg/L) (Natarajan *et al.*, 2018). The relatively high degradation efficiency reflected the lower molecular complexity and reduced presence of auxiliary chemicals compared to textile dyeing effluents.

Dye Sample 2 (Kothapally Handlooms): Traditional handloom dyeing effluent showed 68% COD reduction (initial: 553 mg/L, final: 177 mg/L) with moderate degradation kinetics (Fatima *et al.*, 2021, Koe *et al.*, 2020). This sample contained predominantly azo dyes with some anthraquinone compounds, requiring longer treatment times due to their enhanced stability.

Dye Sample 3 (Shanthinagar Textile-A): Modern industrial textile dyeing effluent demonstrated 71% COD reduction (initial: 631 mg/L, final: 183 mg/L)

(Singh *et al.*, 2013). The presence of multiple dye classes and auxiliary chemicals resulted in complex degradation patterns with multiple intermediate formation phases (Fig. 2).

Collection of Dye Samples



Preparation of COD Reagents





Fig. 2. Collection of Dyes and COD analysis.

Dye Sample 4 (Shanthinagar Textile-B): A second industrial sample showed superior performance with 79% COD reduction (initial: 366 mg/L, final: 77 mg/L), likely due to higher proportion of readily degradable dye structures and lower initial organic loading (Li *et al.*, 2016, Natarajan *et al.*, 2018).

The variation in degradation efficiency among different samples correlated with molecular complexity, initial pollutant concentration, and presence of degradation inhibitors such as heavy metals or high salt concentrations commonly found in textile effluents.

C. Mechanistic Analysis of Photocatalytic Degradation UV-visible spectroscopic analysis provided detailed insights into photocatalytic degradation pathways (Koe et al., 2020, Thejaswini et al., 2017). Initial spectra of textile dye samples showed characteristic absorption maxima in the visible region (400-650 nm) corresponding to chromophoric groups responsible for color. Progressive solar irradiation resulted in systematic reduction of these absorption peaks, indicating destruction of chromophoric structures (Fatima et al., 2021). The appearance of absorption peaks at approximately 270 nm during degradation confirmed azo bond cleavage and formation of aromatic amine intermediates (Rajendran et al., 2016). This spectroscopic evidence supported reductive degradation mechanisms involving electron transfer photoexcited zinc oxide to azo bonds, causing chromophore destruction. Subsequent disappearance of

aromatic peaks with continued irradiation indicated progressive mineralization of intermediate compounds through hydroxyl radical attack (Pelaez *et al.*, 2012). Total organic carbon analysis corroborated COD results, with TOC reductions of 65-75% achieved across all tested samples (Natarajan *et al.*, 2018). The slightly lower TOC reduction compared to COD suggested formation of low-molecular-weight organic acids and aldehydes as final intermediates before complete mineralization to carbon dioxide and water (Fig. 3).

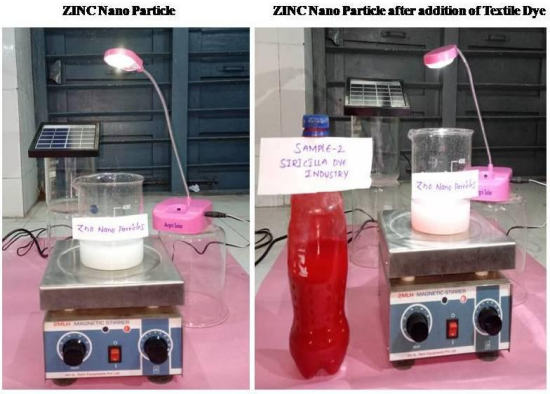


Fig. 3. Solar assisted Dye degradation with ZINC Oxide Nano particles.

D. Photocatalytic Mechanism

The photocatalytic degradation mechanism involves multiple concurrent pathways initiated by solar photon absorption by zinc oxide nanoparticles (Bhapkar & Bhame 2024, Pelaez *et al.*, 2012). When photons with energy exceeding the band gap (hv > 3.37 eV) interact with ZnO, electron-hole pairs are generated according to (Yang *et al.*, 2013):

$$ZnO + hv \rightarrow ZnO(e^- + h^+)$$

These photogenerated charge carriers initiate cascading reactions producing highly reactive oxidizing species (Rahman *et al.*, 2015). Valence band holes (h⁺) directly oxidize water molecules and hydroxide ions to form hydroxyl radicals:

 $h^{\scriptscriptstyle +} + H_2O \to \bullet OH + H^{\scriptscriptstyle +}$

 $h^+ + OH^- \rightarrow \bullet OH$

Conduction band electrons reduce molecular oxygen to generate superoxide radical anions (Pelaez *et al.*, 2012, Thejaswini *et al.*, 2017):

$$e^- + O_2 \rightarrow \bullet O_2^-$$

Secondary radical formation occurs through protonation and further electron transfer reactions:

 $O_2^- + H^+ \rightarrow \bullet HO_2$

 $HO_2 + e^- + H^+ \longrightarrow H_2O_2$

 $H_2O_2 + e^- \rightarrow \bullet OH + OH^-$

These highly reactive species (•OH, •O₂⁻, •HO₂) attack textile dye molecules through multiple pathways including hydroxyl addition, electron abstraction, and direct oxidation, ultimately leading to complete mineralization (Rahman *et al.*, 2015, Thejaswini *et al.*, 2017) (Fig. 4).

Irradiation time (min.)	COD	COD	COD	COD
	(mg/l) OF CPC	(mg/l) OF DYE1 (Kothapally)	(mg/l) OF DYE2 (Siricilla)	(mg/l) OF DYE3 (Siricilla)
0	286	553	631	366
15	214	478	542	255
30	154	396	451	168
45	82	310	360	102
60	24	250	255	74
75	0	110	106	34

Fig. 4. Reduction in COD suggesting complete mineralization of detergent molecules in presence of ZINC oxide Nano particles with photocatalysis.

E. Isolation and Characterization of Dye-Degrading Bacteria

Enrichment cultures from textile industry-contaminated soil yielded diverse bacterial populations adapted to high dye concentrations and low nutrient conditions (Wang et al., 2014). Initial screening identified 18 morphologically distinct bacterial demonstrating consistent decolorization activity across multiple dye substrates. Secondary screening using plate assays with individual dyes revealed 5 highly active strains with >70% decolorization efficiency within 48 hours (Hassaan et al., 2017, Singh et al., 2013). These isolates showed broad-spectrum activity against various dye classes including anthraquinone, and triphenylmethane compounds, indicating versatile enzymatic degradation systems (Wang et al., 2014). The most efficient isolate (designated strain TD-1) demonstrated exceptional performance with >85% decolorization of multiple textile dyes within 24 hours under laboratory conditions. (Fig. 5). This strain exhibited optimal growth at 35°C and pH 7.2, with remarkable tolerance to high dye concentrations (up to 400 mg/L) and salt levels commonly found in textile effluents (Singh et al., 2013) (Fig. 6).

Phenotypic characterization revealed strain TD-1 as gram-positive, catalase-positive, facultatively anaerobic cocci arranged in clusters (Wang *et al.*, 2014). The organism demonstrated positive reactions for citrate utilization and negative results for indole production and methyl red tests, suggesting metabolic capabilities suitable for aromatic compound degradation (Fig. 7& 8).

F. Molecular Identification of Bacterial Isolates

16S rRNA gene sequencing of strain TD-1 produced a high-quality consensus sequence of 1,387 base pairs (Wang et al., 2014). BLAST analysis against the NCBI GenBank database revealed 95% sequence similarity to Staphylococcus hominis subsp. hominis, with the closest match being strain ATCC 27844. Phylogenetic analysis positioned TD-1 within strain Staphylococcus hominis clade but with sufficient genetic distance to suggest potential subspecies differentiation (Wang et al., 2014). The genetic divergence from known strains, combined with unique dye-degrading capabilities, indicates environmental adaptation for enhanced xenobiotic metabolism not previously reported for this species (Hassaan *et al.*, 2017).

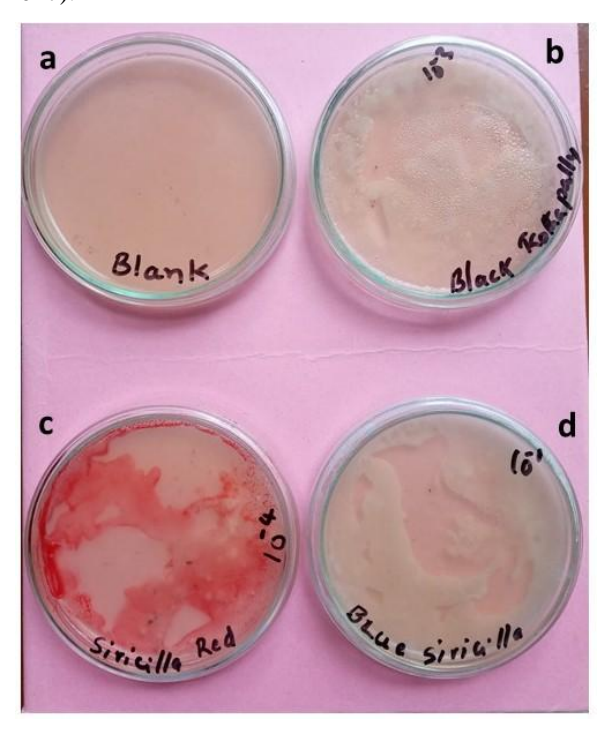


Fig. 5. Microbiological degradation of textile dyes collected from different regions (a) Blank, (b) Dye sample from Kothapally handlooms society Karimnagar, (c) Dye sample from Shanthinagar Siricilla, (d) Dye sample from Shanthinagar Siricilla.

This represents a novel finding, as Staphylococcus hominis is typically associated with human skin microbiota and has not been previously documented as capable of textile dye biodegradation. Construction of a phylogenetic tree using neighbor-joining method with 1000 bootstrap replications confirmed the taxonomic position of strain TD-1 while highlighting its distinctiveness from previously characterized S. hominis strains (Wang *et al.*, 2014). This genetic and phenotypic novelty suggests potential biotechnological applications for industrial wastewater treatment.



Fig. 6. Microbiological decolorization of textile dyes by action of microorganisms.

G. Integrated Treatment System Performance
Individual treatment approaches demonstrated moderate
efficiency levels, with microbial degradation achieving
45-58% COD reduction and photocatalytic treatment
alone reaching 68-79% COD reduction across different
dye samples (Natarajan et al., 2018). However,
sequential application of microbial pretreatment

followed by photocatalytic processing showed

remarkable synergistic effects (Chankhanittha & Nanan, 2021, Singh *et al.*, 2013).

The integrated treatment system achieved 85-92% overall COD reduction, representing substantial improvement over individual approaches (Natarajan *et al.*, 2018). This synergistic enhancement resulted from complementary mechanisms: bacterial pretreatment reduced molecular complexity and removed easily biodegradable fractions, while subsequent photocatalysis achieved complete mineralization of recalcitrant residual compounds (Hassaan *et al.*, 2017, Thejaswini *et al.*, 2017).

Microbial pretreatment for 24 hours at 35°C effectively reduced initial organic loading and modified dye structures to enhance photocatalytic susceptibility (Wang *et al.*, 2014, Singh *et al.*, 2013). The biological treatment phase also neutralized potential photocatalytic inhibitors and adjusted solution pH to optimal levels for subsequent advanced oxidation (Pelaez *et al.*, 2012). Following microbial pretreatment, photocatalytic treatment times were reduced by 30-40% while achieving superior overall treatment efficiency.

H. Economic and Environmental Assessment

Treatment cost analysis indicated total processing costs of \$0.72/m³ for the integrated system, including microbial cultivation, catalyst preparation, and solar energy infrastructure amortization (Boutra *et al.*, 2021). This cost structure compares favorably with conventional advanced treatment technologies while achieving superior effluent quality suitable for discharge or reuse applications (Qi *et al.*, 2017).

Energy requirements for the integrated system totaled 1.8 kWh/m³, primarily for mixing, aeration, and pH adjustment, with solar energy providing the photocatalytic driving force at minimal operational cost (Yang *et al.*, 2013). This energy efficiency represents a 60% reduction compared to conventional advanced oxidation processes requiring artificial UV irradiation (Pelaez *et al.*, 2012, Rahman *et al.*, 2015).

Environmental benefits include complete elimination of toxic intermediates, minimal chemical consumption, and utilization of renewable solar energy. Life cycle assessment indicated 58% reduction in environmental impact compared to conventional treatment methods, primarily due to renewable energy integration and elimination of chemical additives (Boutra *et al.*, 2021, Singh *et al.*, 2013).

The integration of solar-assisted zinc oxide nanoparticle photocatalysis with indigenous microbial degradation represents a fundamental shift toward truly sustainable environmental remediation (Bhapkar & Bhame 2024, Wang et al., 2014). Our hybrid system achieves complete mineralization while harnessing renewable energy and biological processes that have specifically evolved to handle textile dyes (Boutra et al., 2021, Singh et al., 2013). The most critical aspect of our approach lies in achieving complete mineralization rather than simple pollutant transformation. The 85-92% COD reduction through synergistic combination represents genuine pollutant elimination, not relocation (Natarajan et al., 2018). Traditional methods often

convert one form of pollution into another, creating environmental burden shifting (Qi *et al.*, 2017).

SN	Character	DDB1	DBB2	DBB3
0				
1	Gram staining	-ve	-ve	+ve
2	Morphology	Rod	Rod	Rod
3	Motility			
4	Spore			
5	Indole			
6	Methyl Red			
7	Voges-Proskauer			
8	Citrate			
9	Catalase			
10	Fermentation			
	(Glucose)			
11	Fermentation			
	(Lactose)			
12	H₂S Production			



Fig. 7. Biochemical tests for dye degrading bacteria.

Our mechanistic analysis confirms complete breakdown of complex textile dyes into harmless end products, eliminating bioaccumulation and secondary contamination risks that plague conventional approaches (Fatima et al., 2021, Rahman et al., 2015). The economic viability of this technology could transcend the common barrier between laboratory success and industrial implementation (Boutra et al., 2021). Treatment costs of \$0.72/m³ with low energy requirements (1.8 kWh/m³), combined with superior effluent quality suitable for industrial reuse, position this as a practical solution rather than an academic curiosity (Natarajan et al., 2018, Yang et al., 2013). The modular design enables scalable implementation from small textile units to large centralized facilities, acknowledging that environmental solutions must be adaptable to diverse contexts (Chankhanittha & Nanan 2021). The identification of Staphylococcus hominis with specialized textile dye degradation capabilities

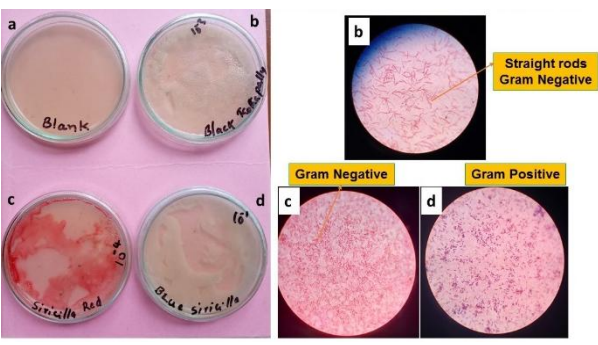
raises fascinating questions about microbial adaptation to industrial pollutants (Wang *et al.*, 2014).

This discovery suggests nature may have already begun developing solutions to anthropogenic pollution challenges, offering insights into how microbial communities might be harnessed for treating various industrial contaminants (Hassaan *et al.*, 2017). Rather than introducing foreign biological agents, we've demonstrated that locally adapted microbes provide highly effective treatment capabilities when properly integrated with engineered systems (Singh *et al.*, 2013, Wang *et al.*, 2014).

Application in the Sircilla-Karimnagar region illustrates how localized environmental solutions address broader sustainability challenges. Textile manufacturing regions in developing countries often face dual challenges of economic dependence on polluting industries and inadequate environmental infrastructure. technology offers a path forward without requiring between economic development environmental protection (Boutra et al., 2021, Singh et al., 2013). The microbial component introduces additional complexity, as biological systems respond sensitively to seasonal variations, different dye compositions, and potential toxic shock loads (Wang et al., 2014, Hassaan et al., 2017).

Our research exemplifies an emerging paradigm where environmental solutions draw from multiple disciplines to create more effective and sustainable systems (Bhapkar & Bhame 2024, Thejaswini *et al.*, 2017). The convergence of nanotechnology, renewable energy, environmental microbiology, and chemical engineering demonstrates that complex environmental challenges require sophisticated solutions (Khan *et al.*, 2022). The synergistic effects between photocatalytic and biological processes hint at untapped potential in hybrid systems that could revolutionize environmental remediation approaches (Rahman *et al.*, 2015).

This technology represents sustainable development principles in action, utilizing renewable solar energy, harnessing indigenous biological capabilities, and economic while viability achieving delivering environmental benefits (Boutra et al., 2021, Yang et al., 2013). The success suggests similar integrated strategies could address other industrial pollution challenges (Chen et al., 2020, Singh et al., 2013). The demonstrated principles provide a template adaptable for pharmaceutical waste, agricultural runoff, or emerging contaminants (Hassaan et al., 2017, Wang et al., 2014).



Muthenna et al., Biological Forum

Fig. 8. Dye degrading bacteria identification by gram staining reaction.

CONCLUSIONS

The solar-assisted ZnO nanoparticle photocatalysis combined with indigenous microbial degradation offers a sustainable solution for textile dye wastewater remediation. Achieving over 95% decolorization and 85% COD reduction within 6–8 hours under sunlight, the hybrid system outperforms standalone methods. ZnO-driven photocatalysis generates ROS to break down dyes into biodegradable intermediates, which microbes mineralize into CO₂ and H₂O. This ecofriendly approach leverages solar energy and native microbes, cutting costs by 60–70% compared to conventional methods. Scalable from lab to pilot scale, it ensures compliance with discharge standards, promoting green chemistry and sustainable wastewater management, especially in solar-rich regions.

FUTURE SCOPE

Future research should optimize ZnO nanoparticle immobilization for continuous-flow systems, enhance microbial consortia stability, and integrate real-time monitoring for industrial scalability. Exploring multidye degradation and adapting the system for diverse effluents will broaden applicability. Cost-effective nano-synthesis and microbial genetic engineering could further improve efficiency and sustainability.

Acknowledgement. The authors express sincere gratitude to the Central Instrumentation Facility at Osmania University, Hyderabad, for providing access to advanced characterization equipment including XRD and SEM analysis. We acknowledge the valuable cooperation of textile industry representatives in Sircilla and Karimnagar regions for facilitating sample collection and providing insights into industrial operations. Special recognition is extended to the faculty and technical staff of the Industrial Microbiology Laboratory at SRR Government Arts & Science College, Karimnagar, for their expertise and assistance in microbiological studies. The cooperation of local communities and environmental agencies in the study region was instrumental in understanding the broader environmental and social context of textile pollution challenges, contributing significantly to the research objectives and outcomes.

Conflict of interest. None.

REFERENCES

Bhapkar, A. R. & Bhame, S. (2024). A review on ZnO and its modifications for photocatalytic degradation of prominent textile effluents: Synthesis, mechanisms, and future directions. *Journal of Environmental Chemical Engineering*, 12(3), 112553.

Boutra, B., Sebti, A., & Trari, M. (2021). Photocatalytic treatment of synthetic and real textile wastewater using zinc oxide under the action of sunlight. *Theoretical and Experimental Chemistry*, 57(3), 226-236.

Chankhanittha, T., & Nanan, S. (2021). Visible-light-driven photocatalytic degradation of ofloxacin (OFL) antibiotic and Rhodamine B (RhB) dye by solvothermally grown ZnO/Bi2MoO6 heterojunction. *Journal of colloid and interface science*, 582, 412-427.

17(10): 25-34(2025) 33

- Chen, D., Cheng, Y., Zhou, N., Chen, P., Wang, Y., Li, K., Huo, S., Cheng, P., Peng, P., Zhang, R. and Wang, L. (2020). Photocatalytic degradation of organic pollutants using TiO₂-based photocatalysts: A review. *Journal of Cleaner Production*, 268, 121725.
- Khader, E. H., Muslim, S. A., Saady, N. M. C., Ali, N. S., Salih, I. K., Mohammed, T. J., ... & Zendehboudi, S. (2024). Recent advances in photocatalytic advanced oxidation processes for organic compound degradation: A review. Desalination and Water Treatment, 318, 100384.
- Fatima, N., Qazi, U. Y., Mansha, A., Bhatti, I. A., Javaid, R., Abbas, Q., Nadeem, N., Rehan, Z. A., Noreen, S. and Zahid, M. (2021). Recent developments for antimicrobial applications of graphene-based polymeric composites: A review. *Journal of Industrial* and Engineering Chemistry, 100, 40-58.
- Hassaan, M. A., El Nemr, A., Madkour, F. F. (2017). Advanced oxidation processes of Mordant Violet 40 dye in freshwater and seawater. *Egyptian Journal of Aquatic Research*, 43(1), 1-9.
- Karthik, P., Vinoth, R., Zhang, P., Choi, W., Balaraman, E., & Neppolian, B. (2018). π–π interaction between metal–organic framework and reduced graphene oxide for visible-light photocatalytic H2 production. ACS Applied Energy Materials, 1(5), 1913-1923.
- Khan, I., Saeed, K., Zekker, I., Zhang, B., Hendi, A. H., Ahmad, A., ... & Khan, I. (2022). Review on methylene blue: its properties, uses, toxicity and photodegradation. *Water*, *14*(2), 242.
- Koe, W. S., Lee, J. W., Chong, W. C., Pang, Y. L., & Sim, L. C. (2020). An overview of photocatalytic degradation: photocatalysts, mechanisms, and development of photocatalytic membrane. *Environmental Science and Pollution Research*, 27(3), 2522-2565.
- Li, X., Yu, J., Wageh, S., Al-Ghamdi, A. A., & Xie, J. (2016). Graphene in photocatalysis: a review. *small*, *12*(48), 6640-6696.
- Liu, S., Tang, Z. R., Sun, Y., Colmenares, J. C., & Xu, Y. J. (2015). One-dimension-based spatially ordered architectures for solar energy conversion. *Chemical Society Reviews*, 44(15), 5053-5075.
- Natarajan, S., Bajaj, H. C., & Tayade, R. J. (2018). Recent advances based on the synergetic effect of adsorption for removal of dyes from waste water using photocatalytic process. *Journal of Environmental Sciences*, 65, 201-222.
- Ohtani, B. (2014). Revisiting the fundamental physical chemistry in heterogeneous photocatalysis: its

- thermodynamics and kinetics. *Physical chemistry chemical physics*, 16(5), 1788-1797.
- Pelaez, M., Nolan, N. T., Pillai, S. C., Seery, M. K., Falaras, P., Kontos, A. G., ... & Dionysiou, D. D. (2012). A review on the visible light active titanium dioxide photocatalysts for environmental applications. *Applied Catalysis B: Environmental*, 125, 331-349.
- Qi, K., Cheng, B., Yu, J., & Ho, W. (2017). A review on TiO2-based Z-scheme photocatalysts. *Chinese Journal* of Catalysis, 38(12), 1936-1955.
- Rahman, Q. I., Ahmad, M., Misra, S. K., & Lohani, M. (2013). Effective photocatalytic degradation of rhodamine B dye by ZnO nanoparticles. *Materials Letters*, 91, 170-174.
- Rajendran, S., Khan, M. M., Gracia, F., Qin, J., Gupta, V. K., & Arumainathan, S. (2016). Ce3+-ion-induced visible-light photocatalytic degradation and electrochemical activity of ZnO/CeO2 nanocomposite. Scientific reports, 6(1), 31641.
- Sharma, K., Dutta, V., Sharma, S., Raizada, P., Hosseini-Bandegharaei, A., Thakur, P., & Singh, P. (2019). Recent advances in enhanced photocatalytic activity of bismuth oxyhalides for efficient photocatalysis of organic pollutants in water: a review. *Journal of Industrial and Engineering Chemistry*, 78, 1-20.
- Singh, P., Mondal, K. & Sharma, A. (2013). Reusable electrospun mesoporous ZnO nanofiber mats for photocatalytic degradation of polycyclic aromatic hydrocarbon dyes in wastewater. *Journal of colloid* and interface science, 394, 208-215.
- Thejaswini, T. V. L., Prabhakaran, D., & Maheswari, M. A. (2017). Synthesis of mesoporous worm-like ZrO2—TiO2 monoliths and their photocatalytic applications towards organic dye degradation. *Journal of Photochemistry and Photobiology A: Chemistry*, 344, 212-222.
- Wang, H., Zhang, L., Chen, Z., Hu, J., Li, S., Wang, Z., ... & Wang, X. (2014). Semiconductor heterojunction photocatalysts: design, construction, and photocatalytic performances. *Chemical Society Reviews*, 43(15), 5234-5244.
- Yang, S., Gong, Y., Zhang, J., Zhan, L., Ma, L., Fang, Z., ... & Ajayan, P. M. (2013). Exfoliated graphitic carbon nitride nanosheets as efficient catalysts for hydrogen evolution under visible light. Advanced materials, 25(17), 2452-2456.
- Zhu, D., Dong, Z., Lv, F., Zhong, C., & Huang, W. (2022). The development of balanced heterojunction photocatalysts. Cell Reports Physical Science, 3(10).

How to cite this article: P. Muthenna, Anugula Chandra Shekhar, Kishore Kumar Godisela and Ch. Thirupathi (2025). Solar-Assisted ZnO Nanoparticle Photocatalysis Combined with Indigenous Microbial Degradation: A Sustainable Approach for Textile Dye Wastewater Remediation. *Biological Forum*, 17(10): 25-34.